Interacting-boson-fermion-approximation description of negative-parity states in even-odd Yb isotopes

S. T. Hsieh
Department of Physics, National Tsing Hua University, Hsinchu, Taiwan, Republic of China

D. S. Chuu
Department of Electrophysics, National Chiao Tung University, Hsinchu, Taiwan, Republic of China
(Received 6 March 1991)

The negative-parity energy levels of the even-odd Yb isotopes, ^{163}Yb, ^{165}Yb, ^{169}Yb, ^{171}Yb, and ^{173}Yb, are studied systematically within the framework of the extended interacting-boson-fermion-approximation (IBFA) model in which one odd fermion is couplied with a boson core. The boson core is described with the IBA model but allowing one boson to break into a quasifermion pair. The odd fermion is assumed to be in one of the $f_{7/2}$ and $p_{3/2}$ single-particle orbitals while the fermion pair is allowed to occupy the single-particle orbit $i_{13/2}$. It was found that the negative-parity energy levels of these even-odd Yb isotopes and the values of transition quadrupole moments for the ground-state rotational band of ^{173}Yb can be reproduced in fairly good agreement with the observed data.

I. INTRODUCTION

Recently, experimental information on even- and odd-mass Yb isotopes has become more abundant [1–17]. These nuclei fall in the transitional region and have several interesting properties. For example, they can assume a variety of shapes [8] ranging from oblate to superdeformed prolate, and thus the coexistence of different nuclear shapes, collective and noncollective rotational modes, is expected. Second, the ytterbium nuclei in this mass region can bear higher angular momentum [1–3,8,11,12]. Furthermore, the energy spacings between the negative-parity levels in some even-odd-mass Yb isotopes have been observed several anomalous phenomena such as the abrupt shrinking [14,15] between some adjacent energy levels and backbendings [3,4] as one plots the moment of inertia versus the square of the angular velocity for yrast band of a nucleus. These phenomena might be a result of the complicated interplay between the collective and single-particle degrees of freedom induced by the Coriolis decoupling [18]. A generalized calculation within the framework of the two-quasiparticle plus rotor band-mixing model [19] predicted that the high-spin states are produced by the alignments of the angular momenta of the decoupled quasiparticles along the collective rotation. Most of the high-spin data can be understood, at least qualitatively, in terms of the cranked shell model [20–22] which assumes aligned high-j nucleons weakly coupled to deformed cores with rather constant deformation parameters. However, the neglect of variations in deformation from state to state is dangerous in the $N=88$–90 transition region between rotational and variational nuclei [9]. Recently, the interacting-boson-approximation (IBA) and interacting-boson-fermion-approximation (IBFA) models including fermion pair degrees of freedom [23–29] were employed to analyze the positive- and negative-parity high-spin anomalies. It was found that high-spin states and the back-bend phenomena could be reproduced quite well.

The negative-parity bands of even-odd-mass Yb isotopes, ^{163}Yb, ^{165}Yb, ^{169}Yb, ^{171}Yb, and ^{173}Yb, are seldom studied in recent years because of their complicated band-crossing patterns. In this work we shall employ the extended IBFA model to study the energy levels of the odd-mass Yb isotopes. These odd-mass nuclei are assumed to be described by an odd fermion weakly coupled to a boson core. The boson core is studied with the extended IBA by allowing one of the bosons to break into a fermion quasiparticle pair, usually assigned to a unique-parity intruder orbital with spin j. In the region of well-deformed nuclei, the unique-parity intruder orbital such as $h_{11/2}$ or $i_{13/2}$ is the most important because both the Coriolis antipairing and rotation alignment effects increase with increasing angular momentum [18,29]. However, a recent study on the negative-parity high-spin states of $N=88$ isotones [30] manifested that the orbit $i_{13/2}$ is the most important one for the first back bending. As a consequence, in this work we restrict the quasiparticle pair to be in the $i_{13/2}$ single-particle orbit only. The odd nucleon for our even-odd-mass isotopes is assumed to distribute in the $f_{7/2}$ or $p_{3/2}$ single-particle orbital. In the present work, the IBA-1 basis states are used in the boson core. This is because the IBA-1 has been proven [31] to be a valid approximation in transitional regions far from the closed shell.

II. MODEL

In the calculation of the negative-parity energy levels of the even-odd-mass Yb isotopes, $Z=N=82$ is taken as the core. The pure IBFA model assumes a valence boson number $N_B=11$, 12, 14, 15, and 16 and a fermion quasiparticle distributed in the single-particle orbitals $f_{7/2}$ or $p_{3/2}$ for the five nuclides ^{163}Yb, ^{165}Yb, ^{169}Yb, ^{171}Yb, and ^{173}Yb, respectively. In addition to the pure IBFA configuration, we admix the N_B-1 boson plus 1 fermion

pair configuration into the model space. To be more specific, the model space is spanned by two types of basis states,

$$|n_s n_d \mu\gamma L, j; J_T M_T\rangle$$

and

$$|[n_s' n_d' \mu'\gamma' L', j'^2(J)]L', j; J_T M_T\rangle \ ,$$

where $n_s+n_d=N_B$, $n_s'+n_d'=N_B-1$, $j=f_{7/2}$ or $p_{3/2}$, $j'=\frac{13}{2}$, and $J\geq 4$. The $J=0$ and 2 fermion pair states are excluded to avoid double counting of the states. The Hamiltonian consists of four parts,

$$H=H_B+H_F+V_{BF}+V_m \ ,$$

where the IBA boson Hamiltonian H_B can be expressed as

$$H_B=a_0 n_d+a_1 P^\dagger\cdot P+a_2 L\cdot L+a_3 Q\cdot Q \ .$$

The octupole term T_3T_3 and hexadecapole term T_4T_4 have been omitted in H_B since they are generally believed to be less important. The fermion Hamiltonian H_F is

$$H_F=\sum_m \varepsilon_j a_{jm}^\dagger a_{jm}+\tfrac{1}{2}V^J(a_j^\dagger a_j^\dagger)^{JM}(\tilde{a}_j\tilde{a}_j)^{JM} \ ,$$

where ε_j is the fermion single-particle energy, the V^J's are the fermion-fermion interactions, and $a_j^\dagger(\tilde{a}_j)$ is the nucleon creation (annihilation) operator.

The boson-fermion Hamiltonian V_{BF} that describes the interaction between the odd quasinucleon and even-even core nucleus contains, in general, many different terms [32] and is rather complicated. However, it has been shown that V_{BF} may very well be approximated by the following three terms [33,34]:

$$V_{BF}=\kappa Q_B\cdot Q_F+\sum_{j,j',k}\Lambda_{jj'}^k:[(a_j^\dagger\times\tilde{d})^{(k)}\times(d^\dagger\times\tilde{a}_{j'})^{(k)}]_0^{(0)}: \ ,$$

where Q_B is the boson quadrupole operator;

$$Q_B=(s^\dagger\times\tilde{d}+d^\dagger\times\tilde{d})^{(2)}+\chi(d^\dagger\times\tilde{d})^{(2)} \ ,$$

and Q_F is the fermion quadrupole operator,

$$Q_F=\sum_{j,j'}\Gamma_{jj'}(a_j^\dagger\times\tilde{a}_{j'})^{(2)} \ ,$$

with

$$\Gamma_{jj'}=(1/\sqrt{5})\langle j\|Y^{(2)}\|j'\rangle \ ,$$

$$\Lambda_{jj'}^k=-\Lambda[(2k+1)/5]^{-1/2}\langle j\|Y^{(2)}\|k\rangle\langle k\|Y^{(2)}\|j'\rangle \ ,$$

and (::) indicates that the commutation of $a_j^\dagger$ and $\tilde{a}_j$ is neglected. The SU(3) value of $\chi=-\sqrt{7}/2$ is adopted in this work. The first term in V_{BF} is a quadrupole-quadrupole interaction, while the second term represents an exchange interaction. The origin of the exchange term is due to the interchange of the odd quasinucleon with one of the nucleons that make up the d boson. The last term in V_{BF} is a monopole interaction, which gives rise to a renormalization of the boson energy $\varepsilon=\varepsilon_d-\Delta$.

The mixing Hamiltonian V_m between the sd boson and quasifermion pair is assumed

$$V_m=\alpha Q_B\cdot(a_j^\dagger\tilde{a}_j)^{(2)}+\beta Q_B\cdot[(a_j^\dagger a_j^\dagger)^{(4)}\tilde{d}-d^\dagger(\tilde{a}_j\tilde{a}_j)^{(4)}]^2 \ .$$

The radial dependence of the fermion potential is taken as the Yukawa type with a Rosenfeld mixture. An oscillation constant $\nu=0.96A^{-1/3}$ fm^{-2} with $A=160$ is assumed. The interaction strength of the V^J's is adjusted by requiring $\langle jj|V|jj\rangle_{j=2}-\langle jj|V|jj\rangle_{j=0}=2$ MeV. The whole Hamiltonian is then diagonalized in the selected model space.

The odd-mass Yb isotopes ^{163}Yb, ^{165}Yb, ^{169}Yb, ^{171}Yb, and ^{173}Yb are assumed as the system with an odd fermion weakly coupled to the even-even boson cores: ^{162}Yb, ^{164}Yb, ^{168}Yb, ^{170}Yb, and ^{172}Yb. To describe the even-even boson core, the fermion pair degrees of freedom are taken into account in the traditional IBA model by allowing a boson to break into one fermion pair which is assumed to distribute in the single-particle orbit $i_{13/2}$. In the practical calculation, the single-particle energy $\varepsilon(i_{13/2})$ and interaction parameters contained in the Hamiltonians H_B and H_m are first chosen to reproduce the positive-parity energy spectra of these five even-even Yb nuclei. After obtaining these parameters, the interaction strengths contained in V_{BF} and the single-fermion energy $\varepsilon(p_{3/2}$-$f_{7/2})$ [the single-particle energy $\varepsilon(f_{7/2})$ is set to be zero] were then fitted to the negative-parity energy spectra of the even-odd Yb nuclei using the following constrains: (1) The single-particle energy of $i_{13/2}$ and interaction parameters contained in H_B and H_m are kept at the same value as those obtained from the fitting of the positive-parity states of even-even Yb nuclei. (2) The parameters κ and Λ are assumed as smooth functions of neutron number. (3) The boson energy ε_d is renormalized as $\varepsilon_d'=\varepsilon_d-\Delta$ due to the strength of the monopole interaction. (4) The fermion single-particle energies for each isotope are allowed to be mass number dependent and are obtained as a result of fitting.

III. RESULTS

The searched interaction strengths for the even-even Yb nuclei are listed in Table I. Note that the mixing parameter β is kept constant for all Yb isotopes. The major effect of the mixing parameter α is to mix the boson-configuration-dominated low-lying states with the fermion pair states. Since the energy-level spacings of the low-lying sates of these five isotopes are different, consequently, the value of the mixing parameter α for each isotopes has to vary to obtain better agreement between the calculated and observed data. The smallness of the mixing parameters α and β manifest in the mixings between the N_B pure boson configurations and N_B-1 boson plus 2 fermion configurations are small, in general, and seem to be consistent with the general analysis of the previous work [19]. The other parameters are all varied monotonically with the mass number. The decreasing of single-boson energy $\varepsilon_d(a_0)$ and the increasing of the strength of $Q\cdot Q$ term (a_3) manifest in the isotopes become more col-

TABLE I. Interaction parameters (in MeV) of the Hamiltonian for even-even Yb nuclei adopted in this work.

Nucleus \ Parameter (MeV)	a_0	a_1	a_2	a_3	α	β	$\varepsilon(i_{13/2})$
^{162}Yb	0.614	0.047	0.0035	−0.0082	0.089	0.03	1.340
^{164}Yb	0.614	0.045	0.0035	−0.0082	0.089	0.03	1.317
^{166}Yb	0.610	0.040	0.0040	−0.0085	0.089	0.03	1.223
^{168}Yb	0.610	0.033	0.0046	−0.0093	0.110	0.03	1.178
^{170}Yb	0.610	0.013	0.0057	−0.0111	0.110	0.03	1.137
^{172}Yb	0.610	0.000	0.0058	−0.0120	0.110	0.03	1.075

lective as the boson number increases. This is consistent with the tendency of deviating away from U(5) symmetry to SU(3) symmetry. Table II lists the interaction parameters of the total Hamiltonian for the even-odd Yb isotopes. The single-particle energy $\varepsilon(i_{13/2})$ and strengths of the $P^{\dagger}\cdot P$ term (a_1), $L\cdot L$ term (a_2), and $Q\cdot Q$ term (a_3) are not shown in Table II because these values are the same as those used in the corresponding even-even cores. The parameter a_0 (ε_d) varied slightly from those of the corresponding even-even core. The variation of a_0 comes from the renormalization due to the monopole-monopole interactions Δ.

The calculated and observed energy spectra for the even-even nuclei ^{162}Yb, ^{164}Yb, ^{168}Yb, ^{170}Yb, and ^{172}Yb are shown in Figs. 1–5. The observed levels with asterisks in Figs. 1 and 2 are not included in the χ-squares fitting because their spin or parity assignments are not quite certain. One can see from the figures that the agreement between the theoretical values and observed data is quite reasonable in general. Recently, the high-spin states of ^{162}Yb have been studied [1] using a ^{127}Sn(^{44}Ca,4n) reaction with a beam of ^{44}Ca ions delivered by the tandem accelerator. Positive-parity states with spin up to 30 are assigned tentatively. Our calculated energy levels shown in Fig. 1 for ^{162}Yb agree fairly well with the observed data and are all in correct order except the 12_2^+ state, which is obtained too low. For ^{164}Yb high-spin states have been populated in the ^{152}Sm(^{16}O,4n) and ^{150}Sm(^{18}O,4n) reactions. The ground-state (g.s.) band and sideband have been established to $I^{\pi}=22^+$ and 26^+. One can note from Fig. 2 that the calculated values are, in general, able to reproduce the observed data fairly well. Figure 3 shows the calculated and experimental energy spectra of ^{168}Yb. The g.s. band can be reproduced quite satisfactorily. However, the shrinking of the adjacent levels in the γ band cannot obtained reasonably. Especially, the 13_1^+ state is obtained too low and thus causes reversed order with its neighboring states. Figures 4 and 5 show the comparisons between the theoretical energy spectra and their experimental counterparts for nuclei ^{170}Yb and ^{172}Yb. The fittings of these two nuclei are very similar to that of ^{168}Yb. Their β and γ bands cannot be reproduced as good as their ground-state bands.

We also analyze the wave function for each state of these even-even Yb isotopes to study the relative intensities of the N_B-pure boson configuration and the N_B-1 boson plus 1 fermion pair configuration. The analysis of the wave functions shows that the states with $I\leq 8^+$ in the g.s. band of the nucleus ^{162}Yb are dominated by the pure boson configuration. The states with $I\geq 16^+$ in the g.s. band are dominated by the configuration of $N-1$ boson plus 2 $i_{13/2}$ fermions. The mixing of these two configurations is only observed in the states 10_1^+ (85.2%–14.8%), 12_1^+ (78.4%–21.6%), and 14_2^+ (55.1%–44.9%). For ^{164}Yb the states with $I\leq 6^+$ are all dominated ($\geq$94%) with the pure boson configuration, while the levels with $I\geq 16^+$ in the g.s. band all states in the sideband are pure N_B-1 boson plus 1 fermion pair configuration except $I=14_2^+$ (8%–92%) and 16_2^+ states (19%–81%). For the g.s band the mixings between these two configurations are only exhibited in the states 8_1^+ (90%–10%), 10_1^+ (85%–15%), 12_1^+ (78%–22%), and 14_1^+ (68%–32%). For ^{168}Yb the pure boson configuration is only dominant in the states with $I\leq 6^+$

TABLE II. Interaction parameters (in MeV) of the total Hamiltonian for even-even Yb nuclei adopted in this work.

Nucleus \ Parameter (MeV)	a_0'	Δ	κ	Λ	$\varepsilon(p_{3/2}-f_{7/2})$
^{163}Yb	0.4738	−0.1401	0.0311	0.2431	−0.5014
^{165}Yb	0.4338	−0.1401	0.0311	0.250	−0.4141
^{169}Yb	0.4425	−0.1645	0.0252	0.531	2.00
^{171}Yb	0.4101	−0.200	0.0199	0.576	2.00
^{173}Yb	0.3542	−0.2558	0.0199	0.7556	3.10

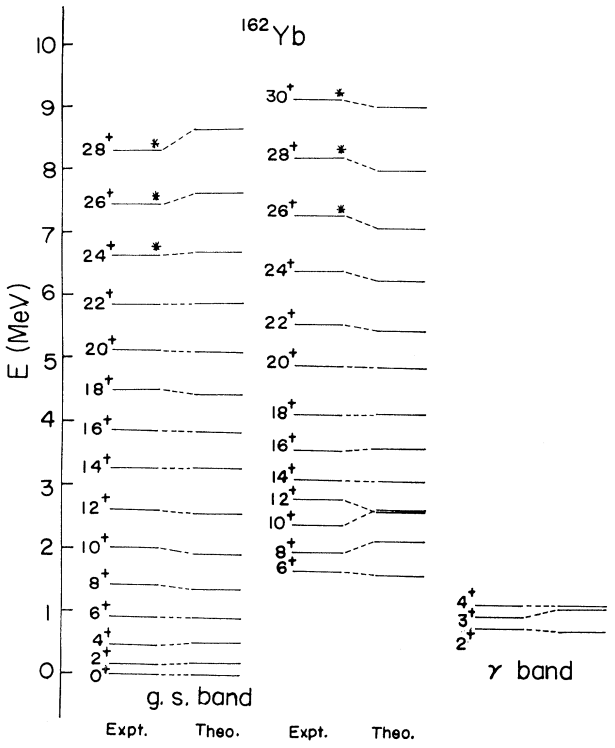

FIG. 1. Calculated and observed energy spectra for the ^{162}Yb nucleus. The experimental data are taken from Ref. [1]. The levels with asterisks are not included in the χ-squares fitting.

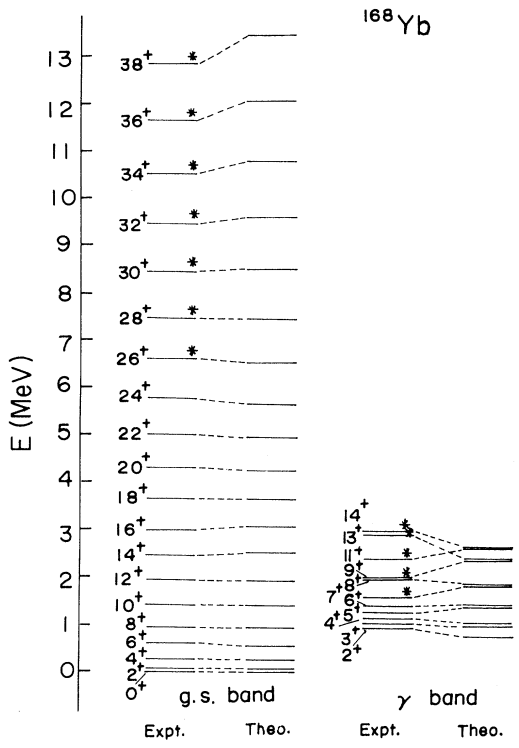

FIG. 3. Calculated and observed energy spectra for the ^{168}Yb nucleus. The experimental data are taken from Ref. [5]. The levels with asterisks are not included in the χ-squares fitting.

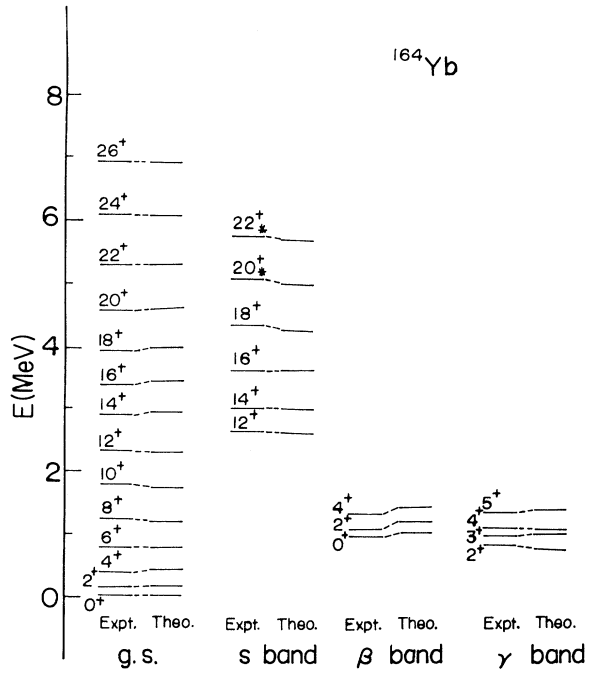

FIG. 2. Calculated and observed energy spectra for the ^{164}Yb nucleus. The experimental data are taken from Ref. [2]. The levels with asterisks are not included in the χ-squares fitting.

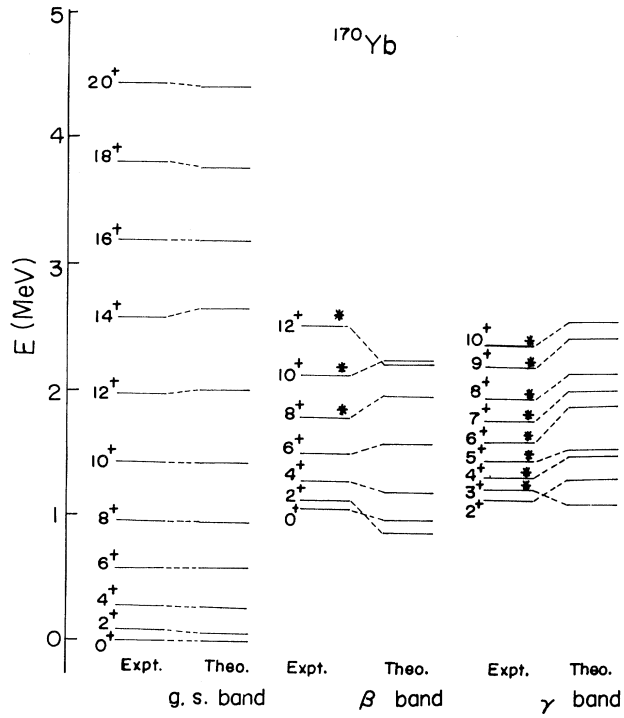

FIG. 4. Calculated and observed energy spectra for the ^{170}Yb nucleus. The experimental data are taken from Ref. [6]. The levels with asterisks are not included in the χ-squares fitting.

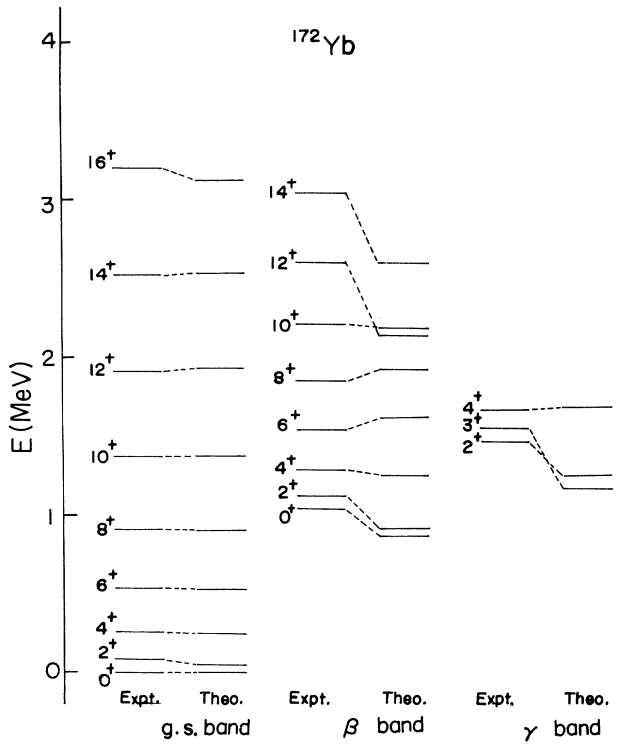

FIG. 5. Calculated and observed energy spectra for the ^{172}Yb nucleus. The experimental data are taken from Ref. [7].

in the g.s. band $I \leq 7^+$ in the γ band. The states with $I \geq 16^+$ in the g.s. band $I \geq 11^+$ in the γ band are all dominated with the configuration of $N-1$ boson plus 2 $i_{13/2}$ fermion. The mixing of these two configurations is prominent only in the states 8_1^+ (86.7%–13.3%), 8_2^+ (71.3%–28.7%), 10_1^+ (78.9%–21.1%), 12_1^+ (68%–32%), and 14_1^+ (53%–47%). For the nuclei ^{170}Yb and ^{172}Yb, the relative intensities of the pure boson and one-fermion pair excitation configurations of the wave function for each state are listed in the Tables III and IV. One can note from the tables that in terms of the relative intensity these states are more dispersive.

The calculated and observed negative-parity energy spectra for odd-mass ^{163}Yb, ^{165}Yb, ^{169}Yb, ^{171}Yb, and ^{173}Yb isotopes are shown in Figs. 6–11. The levels marked with asterisks are not included in the fitting. The dashed levels are the predictions for those yet unobserved levels. There are abundant experimental data observed [6–17] in recent years. For example, Beck *et al.* [3] used the advent of Compton-suppressed multidetector arrays to analyze the triple γ-ray coincidence spectra. The negative-parity level scheme of ^{165}Yb up to $\frac{77}{2}^-$ was assigned. In Figs. 6–9 the different quasibands are displayed in different columns for clear comparison. For the nucleus ^{173}Yb, only the yrast band is presented due to scarce and uncertain observed data. One can see from the figures that the calculated energy levels including in the χ-squares fitting for odd-mass Yb isotopes agree in general reasonably well with the observed data especially

TABLE III. Relative intensities of wave functions for energy levels of the ^{170}Yb and ^{172}Yb nuclei.

Nucleus	^{170}Yb		^{172}Yb	
states	0	$i^2_{13/2}$	0	$i^2_{13/2}$
0_1	0.979	0.021	0.977	0.023
2_1	0.958	0.042	0.935	0.047
4_1	0.944	0.056	0.936	0.064
6_1	0.914	0.086	0.904	0.096
8_1	0.862	0.138	0.849	0.151
10_1	0.782	0.218	0.768	0.232
12_1	0.666	0.334	0.656	0.344
14_1	0.452	0.548	0.509	0.491
16_1	0.001	0.999	0.006	0.994
18_1	0.000	1.000		
20_1	0.000	1.000		
0_2	0.959	0.041	0.959	0.041
2_2	0.962	0.038	0.957	0.043
4_2	0.936	0.064	0.918	0.082
6_2	0.862	0.138	0.745	0.255
8_2	0.361	0.639	0.220	0.780
10_2	0.098	0.902	0.099	0.901
12_2	0.000	1.000	0.000	1.000
14_2	0.075	0.925	0.009	0.991
2_3	0.954	0.046	0.952	0.048
3_1	0.942	0.058	0.928	0.072
4_3	0.843	0.157	0.651	0.349
5_1	0.939	0.061	0.921	0.079
6_3	0.194	0.806	0.302	0.698
7_1	0.894	0.106	0.797	0.203
8_3	0.551	0.449	0.122	0.878
9_1	0.007	0.993	0.005	0.995
10_3	0.019	0.981	0.000	1.000
12_3	0.070	0.930	0.000	1.000
14_3	0.064	0.936	0.000	1.000

for the g.s band. Figures 6 and 7 show the calculated and observed energy spectra of ^{163}Yb and ^{165}Yb. One can note that the calculated levels for these two isotopes are all in correct order and agree reasonably with their experimental counterparts, except for very few levels, e.g., the $\frac{7}{2}^-$ and $\frac{11}{2}^-$ states in ^{163}Yb and the $\frac{11}{2}^-$ state in ^{165}Yb. For these states the theoretical level energies obtained are too low. We also present some experimental unobserved states such as the $\frac{15}{2}^-$, $\frac{19}{2}^-$, and $\frac{23}{2}^-$ states in ^{163}Yb and the $\frac{15}{2}^-$, $\frac{19}{2}^-$, $\frac{23}{2}^-$, $\frac{27}{2}^-$, and $\frac{71}{2}^-$ states in ^{165}Yb for future experimental reference. Figures 8 and 9 present the theoretical and experimental energy levels for ^{169}Yb and ^{171}Yb. One can note from the figures that the calculated $\frac{1}{2}^-$ state in ^{169}Yb and ^{171}Yb obtained is too high. We need a rather strong exchange interaction in order to lower the calculated excitation energy of the $\frac{1}{2}^-$ state, which is the bandhead of the ground-state band. However, the strong exchange interaction will make the agreement between the calculated and observed energy spectra become worse. From Figs. 8 and 9 one can also note that anomalous phenomena such as the abrupt shrinking of the energy spacings between two adjacent energy levels (signature properties) observed in the $\frac{1}{2}[521]$ band of nuclei ^{169}Yb and ^{171}Yb can be reproduced reasonably. Fig-

ure 10 shows the calculated and observed energy differences between two adjacent levels, $\Delta E(I)=E(I)-E(I-1)$, of the ground-state band $\frac{1}{2}[521]$ for isotopes ^{169}Yb and ^{171}Yb. One can note from the figure that the observed zigzag lines (signature dependence) can be fairly well reproduced. Figure 11 shows the calculated and observed energy spectra of ^{173}Yb. Yoshida *et al.* [26] studied the signature dependence of the energy levels and $M1$ and $E2$ transitions in ^{173}Yb in terms of the interacting boson-fermion model. This nucleus was considered as a system of an odd fermion coupled with the boson core ^{172}Yb described by IBA. In the work of Yoshida *et al*; the fermion pair degrees of freedom are not taken into account for the boson core; hence the high-spin states can only be reproduced qualitatively. On the contrary, one can see from Fig. 11 that the high-spin levels can be reproduced reasonably well. In order to investigate the contributions of the interaction parameters κ ($Q_B \cdot Q_F$ term) and Λ (the exchange term), we set these two parameters to be zero alternatively. The energy spectra obtained by setting $\kappa=0$ or $\lambda=0$ are presented also in the Fig. 11. It can be seen that a zero Λ lowers the energy levels significantly, while a zero value of κ can make only a slight deviation from the original result.

We also calculate the relative intensities of the wave functions for each energy level corresponding to $f_{7/2}$ and $p_{3/2}$ single-fermion orbitals for the odd-mass Yb isotopes. It is found that all states of ^{169}Yb, ^{171}Yb, and ^{173}Yb are dominated by the $f_{7/2}$ single-particle orbital with intensity greater than 96%. However, the intensities of the wave functions for the energy level in the nuclei ^{163}Yb and ^{165}Yb are rather dispersive. Table III lists the rela-

TABLE IV. Relative intensities of wave functions for energy levels of the ^{163}Yb and ^{165}Yb nuclei.

Nucleus	^{163}Yb			^{165}Yb	
State	$f_{7/2}$	$p_{3/2}$	State	$f_{7/2}$	$p_{3/2}$
$(\frac{5}{2})_1$	0.435	0.565	$(\frac{5}{2})_1$	0.569	0.431
$(\frac{3}{2})_1$	0.131	0.869	$(\frac{7}{2})_1$	0.194	0.806
$(\frac{7}{2})_1$	0.140	0.860	$(\frac{9}{2})_1$	0.599	0.401
$(\frac{9}{2})_1$	0.489	0.511	$(\frac{11}{2})_1$	0.263	0.737
$(\frac{11}{2})_1$	0.198	0.802	$(\frac{13}{2})_1$	0.688	0.312
$(\frac{13}{2})_1$	0.602	0.398	$(\frac{15}{2})_1$	0.307	0.693
$(\frac{15}{2})_1$	0.238	0.762	$(\frac{17}{2})_1$	0.769	0.231
$(\frac{17}{2})_1$	0.709	0.291	$(\frac{19}{2})_1$	0.368	0.632
$(\frac{19}{2})_1$	0.292	0.708	$(\frac{21}{2})_1$	0.859	0.141
$(\frac{21}{2})_1$	0.832	0.168	$(\frac{23}{2})_1$	0.510	0.490
$(\frac{23}{2})_1$	0.420	0.580	$(\frac{25}{2})_1$	0.119	0.881
$(\frac{23}{2})_2$	0.119	0.881	$(\frac{27}{2})_1$	0.404	0.596
$(\frac{25}{2})_1$	0.103	0.897	$(\frac{29}{2})_1$	0.119	0.881
$(\frac{25}{2})_2$	0.838	0.162	$(\frac{31}{2})_1$	0.417	0.583
$(\frac{27}{2})_1$	0.322	0.678	$(\frac{33}{2})_1$	0.122	0.878
$(\frac{29}{2})_1$	0.103	0.897	$(\frac{35}{2})_1$	0.122	0.878
$(\frac{29}{2})_2$	0.070	0.930	$(\frac{37}{2})_1$	0.125	0.875
$(\frac{31}{2})_1$	0.104	0.896	$(\frac{39}{2})_1$	0.126	0.874
$(\frac{33}{2})_1$	0.105	0.895	$(\frac{41}{2})_1$	0.128	0.872
$(\frac{33}{2})_2$	0.065	0.935	$(\frac{43}{2})_1$	0.135	0.865
$(\frac{35}{2})_1$	0.106	0.894	$(\frac{45}{2})_1$	0.132	0.868
$(\frac{37}{2})_1$	0.108	0.892	$(\frac{47}{2})_1$	0.228	0.772
$(\frac{37}{2})_2$	0.106	0.894	$(\frac{49}{2})_1$	0.135	0.865
$(\frac{39}{2})_1$	0.109	0.891	$(\frac{51}{2})_1$	0.306	0.694
$(\frac{41}{2})_1$	0.111	0.889	$(\frac{53}{2})_1$	0.139	0.861
$(\frac{43}{2})_1$	0.115	0.885	$(\frac{55}{2})_1$	0.333	0.667
$(\frac{45}{2})_1$	0.114	0.886	$(\frac{57}{2})_1$	0.260	0.740
$(\frac{47}{2})_1$	0.210	0.790	$(\frac{59}{2})_1$	0.359	0.641
			$(\frac{61}{2})_1$	0.272	0.728
			$(\frac{63}{2})_1$	0.378	0.622
			$(\frac{65}{2})_1$	0.252	0.748
			$(\frac{67}{2})_1$	0.378	0.622
			$(\frac{69}{2})_1$	0.203	0.797
			$(\frac{71}{2})_1$	0.634	0.366
			$(\frac{73}{2})_1$	1.000	0.000

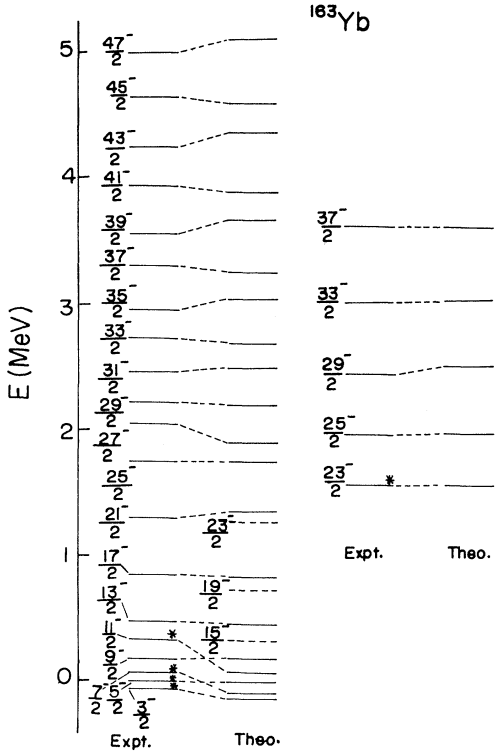

FIG. 6. Calculated and observed energy spectra for the ^{163}Yb nucleus. The experimental data are taken from Ref. [11]. The levels in dashed lines are the predicted energy levels. The levels with asterisks are not included in the χ-squares fitting.

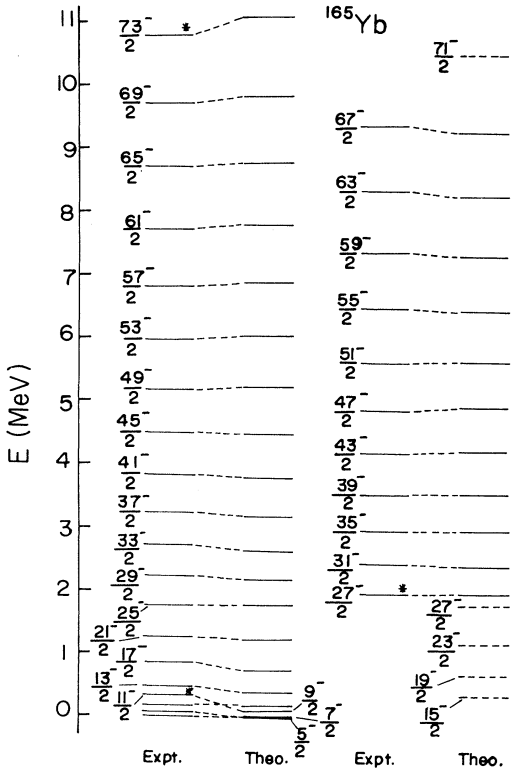

FIG. 7. Calculated and observed energy spectra for the ^{165}Yb nucleus. The experimental data are taken from Refs. [12] and [13]. The levels in dashed lines are the predicted energy levels. The levels with asterisks are not included in the χ-squares fitting.

tive intensities of the wave functions for these two nuclei. One can see from the table that the mixing of $f_{7/2}$ and $p_{3/2}$ single-particle orbitals is prominent in most of the states in these two nuclei.

For ^{173}Yb there is experimental information on the transition quadrupole moment [17]. The study of these values provides us a good test of the model wave functions. The electric quadrupole operator can be written as

$$T(E2)=e^B Q_B+e^F\alpha(a_j^\dagger\times\tilde{a}_j)^{(2)}$$
$$+\beta e^B[(a_j^\dagger\times a_j^\dagger)^{(4)}\times\tilde{d}-d^\dagger\times(\tilde{a}_j\times\tilde{a}_j)^{(4)}]^{(2)}\ .$$

For the fermion effective charge e^F, an average value $0.37e$ of the proton and neutron obtained by Alonso, Arias, and Lozano [28] is adopted. The boson effective charge in the $T(E2)$ operator is assumed to be $0.22e$, which is close to the value used in the previous work [35].

The $\Delta I=1$ and 2 transition quadrupole moments for the ground-state rotational band of ^{173}Yb are defined as

$$Q^{(\Delta I)}=\{B(E2;I\rightarrow I-\Delta I)/[(5/16\pi)\langle I2K0|I$$
$$-\Delta IK\rangle^2]\}^{1/2}\ ,$$

where $K=\frac{5}{2}$ was assumed. The parameters α and β are assumed the same values as used in the mixing Hamil-

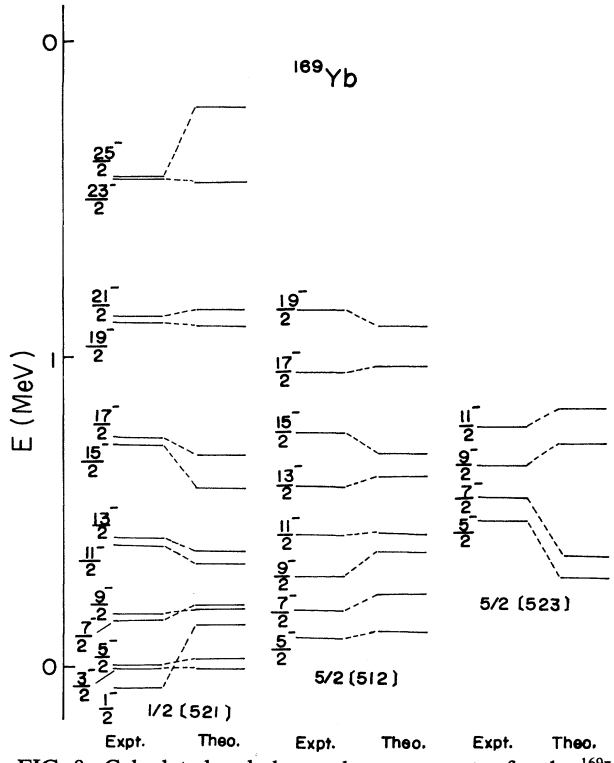

FIG. 8. Calculated and observed energy spectra for the ^{169}Yb nucleus. The experimental data are taken from Ref. [15].

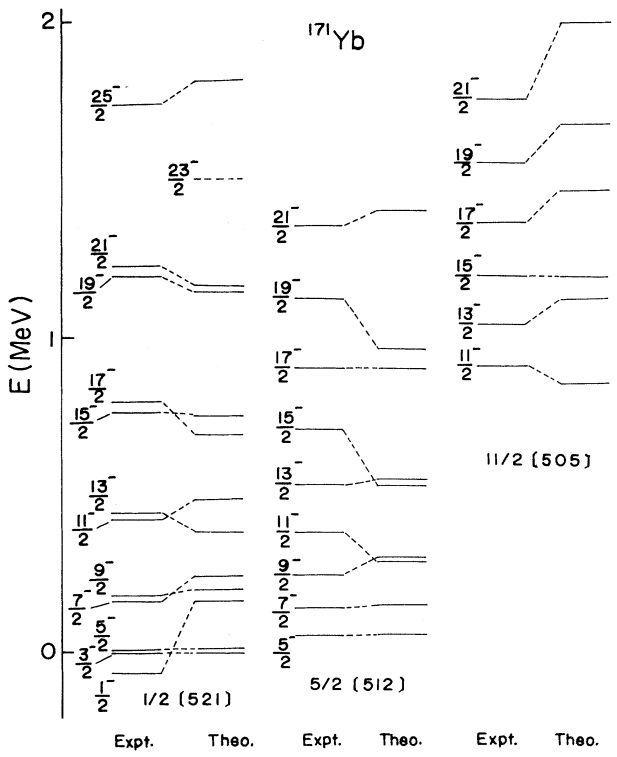

FIG. 9. Calculated and observed energy spectra for the ^{171}Yb nucleus. The experimental data are taken from Ref. [16]. The levels in dashed lines are the predicted energy levels.

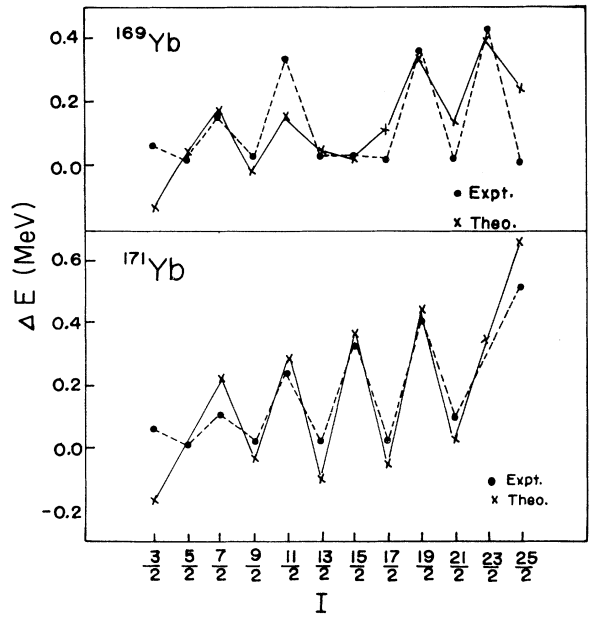

FIG. 10. Calculated and observed energy differences $\Delta E(I)=E(I)-E(I-1)$ for the nuclei ^{169}Yb and ^{171}Yb. The experimental data are taken from Refs. [15] and [16], respectively. The dashed lines represent the observed values, while the solid lines represent the calculated values in this work.

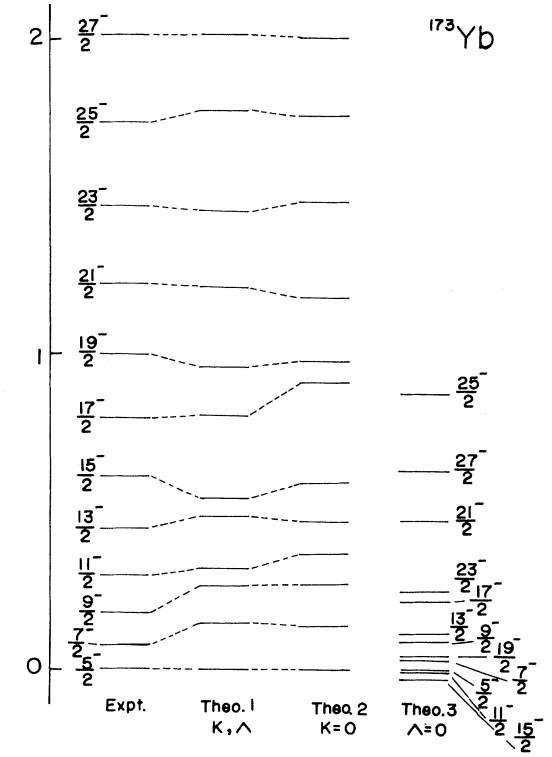

FIG. 11. Calculated and observed energy spectra for the ^{173}Yb nucleus. The experimental data are taken from Ref. [17].

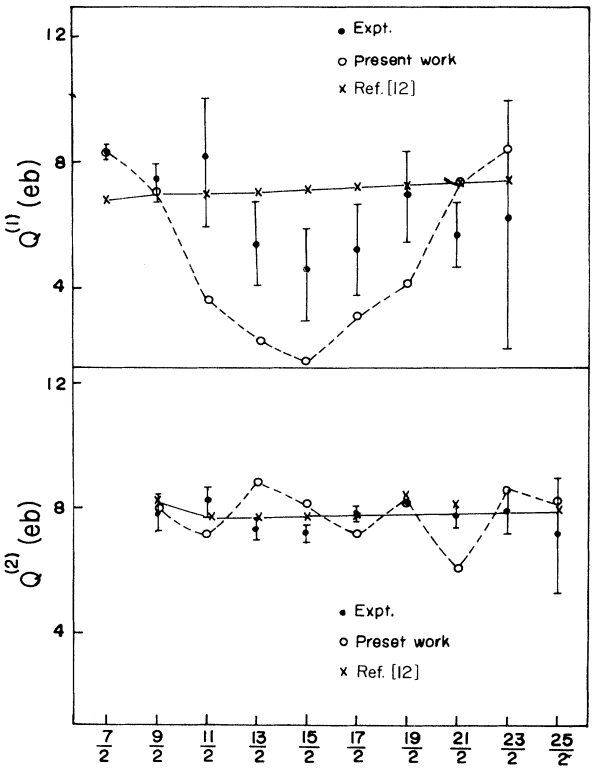

FIG. 12. Calculated and observed transition quadrupole moments for the ^{173}Yb nucleus. The experimental data are taken from Ref. [18] and references therein. The dashed curves represent the results obtained in this work, and the solid curve is obtained by Ref. [18].

tonian. Since the structure of ^{173}Yb is close to SU(3) symmetry, the value of χ is chosen to be $-\sqrt{7}/2$, which is the value for the SU(3) group generator. Figure 12 shows the calculated and observed transition quadrupole moments versus the spins of the depopulating states. From the figure it can be seen that the parabolic formlike feature of $Q^{(\Delta I=1)}$ from spin $\frac{11}{2}^-$ to $\frac{19}{2}^-$ and the fine variation feature of $Q^{(\Delta I=2)}$ can be reproduced qualitatively, especially when the dip occurs at $I=\frac{15}{2}^-$, although our calculated values exaggerate the dip at $I=\frac{15}{2}^-$ and yield a somewhat larger $Q^{(\Delta I=1)}$ value at $I=\frac{21}{2}^-$. On the contrary, the previous works of Oshima *et al.* [17] with the rotating shell model and Yoshida *et al.* [26] with the IBFA model can only obtain nearly flat curves.

IV. SUMMARY AND DISCUSSION

In summary, we have investigated the negative-parity states of the odd-mass ytterbium nuclei in the framework of the extended interacting boson-fermion model. These nuclei are described by coupling an odd fermion to the even-even core. The core is described by the IBA Hamiltonian with the fermion pair degrees of freedom being taken into account. That is, one of the bosons is allowed to break into a fermion pair which can occupy the $i_{13/2}$ single-fermion orbit. The odd quasinucleon is allowed to occupy the $2p_{3/2}$ or $1f_{7/2}$ single-particle orbitals. The parameters contained in the core Hamiltonian are chosen to reproduce the positive-energy spectra of the corresponding even-even Yb isotopes. With this set of parameters, the strengths of odd fermion single-particle energies and the parameters contained in the fermion Hamiltonian are then chosen to reproduce the energy spectra of the even-odd Yb isotopes. The calculated energy levels for the even-even nuclei and even-odd Yb nuclei are all in reasonable agreement with the observed values. Although the observed transition quadrupole moments in the odd-mass Yb region are not abundant, our calculation yields good agreement with the observed values. We also analyzed the intensities of the wave functions corresponding to each single-nucleon orbital for each state. It is found that the intensities of the wave functions for states of ^{163}Yb and ^{165}Yb isotopes are rather dispersive.

This work is supported by the National Science Council of ROC under the Grant No. NSC80-0208-M009-13.

[1] J. N. Mo, S. Sergiwa, R. Chapman, J. C. Lisle, E. Paul, J. C. Willmott, J. Hattula, M. Jääskeläinen, J. Simpson, P. M. Walkert, J. D. Garrett, G. B. Hagemann, B. Herskind, M. A. Riley, and G. Sletten, Nucl. Phys. **A472**, 295 (1987).
[2] S. Jonsson, N. Roy, H. Ryde, W. Walus, J. Kownaccki, J. D. Garrett, G. B. Hagemann, B. Hersind, R. Bengtsson, and S. Åberg, Nucl. Phys. **A449**, 537 (1986).
[3] E. M. Beck, J. C. Bacelar, M. A. Deleplanque, R. M. Diamond, F. S. Stephens, J. E. Draper, B. Herskind, A. Holm, and P. O. Tjøm, Nucl. Phys. **A464**, 472 (1987).
[4] A. E. Ignatochkin, E. N. Shurshikov, and Yu. F. Jaborov, Nucl. Data Sheets **52**, 365 (1987).
[5] V. S. Shirley, Nucl. Data Sheets **53**, 223 (1988).
[6] C. Zhou, Nucl. Data Sheets **50**, 351 (1987).
[7] G. Wang, Nucl. Data Sheets **51**, 577 (1987).
[8] T. Byrski, F. A. Beck, J. C. Merdinger, A. Nourreddine, H. W. Cranmer-Gordon, D. V. Elenkov, P. D. Forsyth, D. Howe, M. A. Riley, J. F. Sharpey-Schafer, J. Simpson, J. Dudek, and W. Nazarewicz, Nucl. Phys. **A474**, 193 (1987).
[9] M. P. Fewell, N. R. Johnson, F. K. Mcgowan, J. S. Hattula, I. Y. Lee, C. Baktash, Y. Schutz, J. C. Wells, L. L. Riedinger, M. W. Guidry, and S. C. Pancholi, Phys. Rev. C **37**, 101 (1988).
[10] R. G. Helmer, Nucl. Data Sheets **43**, 1 (1984).
[11] T. W. Burrows, Nucl. Data Sheets **56**, 313 (1989).
[12] L. K. Peker, Nucl. Data Sheets **50**, 137 (1987).
[13] B. Harmatz, Nucl. Data Sheets **17**, 143 (1976).
[14] V. S. Shirley, Nucl. Data Sheets **36**, 443 (1982).
[15] V. S. Shirley, Nucl. Data Sheets **43**, 127 (1984).
[16] V. S. Shirley, Nucl. Data Sheets **54**, 589 (1988).
[17] M. Oshima, M. Matsuzaki, S. Ichikawa, H. Iimura, H. Kusakari, T. Inamura, A. Hashizume, and M. Sugawara, Phys. Rev. C **40**, 2084 (1989).
[18] F. S. Stephens and R. S. Simon, Nucl. Phys. **A183**, 257 (1972).
[19] C. Flaum and D. Cline, Phys. Rev. C **14**, 1224 (1976).
[20] R. Bengtsson and S. Frauendorf, Nucl. Phys. **A314**, 27 (1979); **A327**, 139 (1979).
[21] Y. S. Chen, S. Frauendorf, and L. L. Riedinger, Phys. Lett. B **171**, 7 (1986).
[22] M. W. Guidry, C-L. Wu, Z.-P. Li, D. H. Feng, and J. N. Ginocchio, Phys. Lett. B **187**, 210 (1987).
[23] A. Arima and F. Iachello, Phys. Rev. Lett. **35**, 1069 (1975); **40**, 385 (1978); Ann. Phys. (N.Y.) **99**, 253 (1976); **111**, 201 (1978); **121**, 468 (1979).
[24] A. Gelberg and A. Zemel, Phys. Rev. C **22**, 937 (1980).
[25] I. Morrison, A. Faessler, and C. Lima, Nucl. Phys. **A372**, 13 (1981).
[26] N. Yoshida, H. Sagawa, T. Otsuka, and A. Arima, Nucl. Phys. **A503**, 90 (1989).
[27] N. Yoshida and A. Arima, Phys. Lett. **164B**, 231 (1985).
[28] C. E. Alonso, J. M. Arias, and M. Lozano, Phys. Lett. B **177**, 130 (1986).
[29] D. S. Chuu and S. T. Hsieh, Phys. Rev. C **38**, 960 (1988).
[30] D. S. Chuu, S. T. Hsieh, and M. M. K. Yen, Prog. Theor. Phys. **85**, 271 (1991).
[31] H. Harter, A. Gelberg, and P. Von Brentano, Phys. Lett. B **157**, 1 (1988).
[32] A. Arima and F. Iachello, in *Advances in Nuclear Physics,* edited by J. W. Negele and E. Vogt (Plenum, New York, 1984), Vol. 13, p. 139.
[33] F. Iachello and O. Scholten, Phys. Rev. Lett. **43**, 679 (1979).
[34] J. Gizon, A. Gizon, and J. Meyer-ter-Vehn, Nucl. Phys. **A277**, 464 (1977).
[35] D. S. Chuu and S. T. Hsieh, Nucl. Phys. **A496**, 45 (1989).